

Preparation, hydrothermal stability and thermal adsorption storage properties of binderless zeolite beads

Jochen Jänchen^{1*}, Kristin Schumann², Erik Thrun³, Alfons Brandt², Baldur Unger² and Udo Hellwig¹

¹Technical University of Applied Sciences Wildau, Bahnhofstraße, 15745 Wildau, Germany; ²Chemiewerk Bad Köstritz GmbH, Heinrichshall 2, 07586 Bad Köstritz, Germany; ³ZeoSolar e.V., Volmerstr. 13, 12489 Berlin, Germany

Abstract

Novel binderless zeolite beads of types A and X have been synthesized and characterized by scanning electron microscopy, mercury intrusion, nitrogen adsorption, thermogravimetry, water adsorption isotherm measurements, cyclic hydrothermal treatments and storage tests. The binderless molecular sieves show an improved adsorption capacity, sufficient hydrothermal stability, higher specific energies and the potential for a better performance density of the storage. Both open and closed storage tests have shown comparable adsorption capacities and specific energies for the binderless molecular sieves. A significantly higher discharging temperature, however, could be realized with the open storage system.

Keywords: zeolite; thermochemical storage; water adsorption; hydrothermal stability

Received 1 March 2012; revised 20 March 2012; accepted 29 March 2012

*Corresponding author:
jochen.jaenchen@th-wildau.de

1 INTRODUCTION

New or modified zeolites have been asked for application in thermal-driven heat pumps or thermochemical storages to improve their performance. These technologies become more and more important in a changing world towards energy conservation, low carbon energy supply and finally, increasing implementation of renewable energies. A number of researchers [1–5] have been active already in developing and characterizing adjusted zeolitic materials for this purpose in the last decade.

We continued in this field to develop a new technology to manufacture molecular sieve beads without a binder by transforming the generally necessary binder into zeolite to enhance the performance and storage capacity for those applications in the energy technology.

The aim of this article is to compare the adsorption properties and hydrothermal behaviour of both the binderless and the binder-containing molecular sieves with respect to the texture, the water adsorption capacities, the hydrothermal stability under cyclic conditions and the thermochemical storage properties in open [6, 7] and closed systems.

2 EXPERIMENTAL STUDY

2.1 Materials and methods

Different types of molecular sieve beads with a binder, the standard molecular sieves 4AK and 13XK, as well as the new binderless materials 4ABF and 13XBF have been investigated in this study.

A number of physicochemical methods have been employed to examine their properties such as scanning electron microscopy (SEM), mercury intrusion, nitrogen adsorption, thermogravimetry (TG), water isotherm measurements, cyclic hydrothermal treatments close to conditions in open and closed systems and storage tests.

The adsorption and storage properties of the zeolites have been studied by TG with a heating rate of 3 K/min after hydration at controlled humidity (33%) and room temperature in an exsiccator. Gravimetric isotherm measurements have been carried out in a vacuum system using a McBain balance at 298–368 K and 0.001–30 mbar water vapour pressure. Prior to the isotherm experiments, the samples (~100–150 mg) were calcined at 623 K.

2.2 Preparation of the zeolite beads

The synthesis of the binderless molecular sieves starts with mixing of zeolite powder (4A or 13X), metakaolin, caustic and silica in the case of zeolite 13X and forming of beads. These so-called crude beads are dried and/or aged to convert the metakaolin into zeolite (Figure 1).

The outcome is a shaped material, consisting of 100% zeolite (4A or 13X) and, if desired, may undergo an ion exchange thereafter (i.e. to form 3A). Finally, the material has been washed, dried and calcined.

Two different types of zeolite morphologies have been obtained by the conversion of the metakaolin. The outer surface of the beads shows typical zeolite crystals (Figure 1), whereas the interior of the beads exhibits unusual polycrystalline structures but consisting of zeolite (not shown) [8]. This observation is most probably due to the formation of zeolite phases in dense matter. Further, the binderless molecular sieves contain mainly macro pores as a secondary pore system. The amount of mesopores in XBF is reduced from initially 30% in

binder-containing zeolite beads to 5% in the binderless ones due to results of the N₂ adsorption and mercury intrusion [8].

2.3 Thermal adsorption storage

The open storage consists of a vaporizer delivering an airstream of controlled humidity connected to the main body of the storage hosting the storage material of ~1.5 l volume. Figure 2 shows the main parts of the storage. A condenser and an adjustable exhauster complete the lab-scaled storage. The apparatus is equipped with sensors for temperature, humidity and air flux measurements as well as a data logger and a computer.

The closed storage unit with a volume of ~1.5 l as well consists of an adsorber filled with ~1 kg of the storage material covering a heat exchanger. The heat exchanger is connected to a thermostat/pump for heat transfer in the charging and discharging mode. The storage is connected with an evaporator (for discharging), a condenser with a chiller for charging (desorption of water) and a vacuum pump. The set-up is equipped with pressure sensors, thermocouples and data acquisition. The heat generated during discharging the thermochemical storage was transferred via a heat exchanger into a water reservoir of 7 l volume. The maximum charging temperature amounts to 473 K. The minimum temperature in the condenser was 274 K. For discharging of the storage, the temperature of the evaporator was kept at ~293 K.

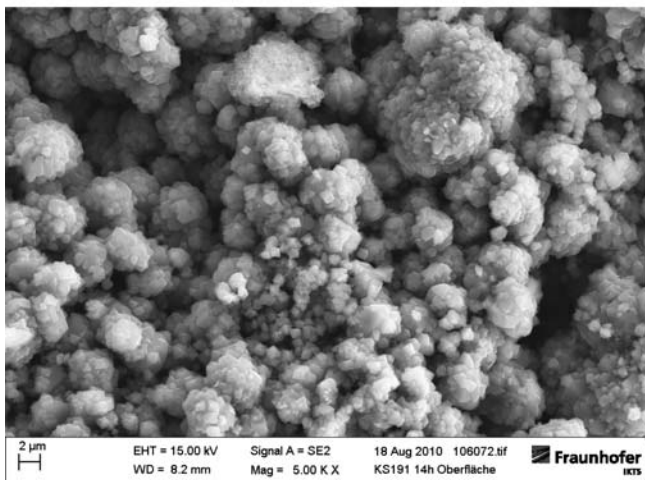
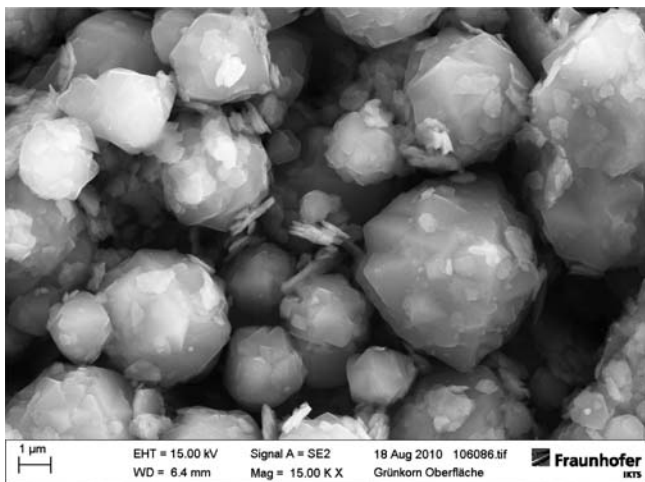


Figure 1. SEM images of the crude beads of 13X zeolite powder mixed with metakaolin (plates, top) and of the surface of binderless 13XBF beads after conversion of the binder (bottom).

3 RESULTS AND DISCUSSION

Table 1 gives a comparison of the adsorption capacities of the A- and X-zeolite types without and with a binder. Column 2 in Table 1 gives the adsorbed amount at relative humidity (RH) = 33% from isotherm measurements upon activation (desorption) at 623 K. Striking is the difference between the binderless samples and the standard zeolites of each type. As expected, a water amount of ~12–15% less can be stated for the standard zeolites verified by TG results (column 3 in Table 1) and Figure 3 (water adsorption isotherms).

Figure 3 shows the isotherm of the molecular sieves in the adsorption and desorption mode. As can be seen, all isotherms in Figure 3 are completely reversible, indicating measurements at true equilibrium conditions. However, the time to get equilibrium values was significantly shorter for the binderless samples.

In particular, for 13XBF, mass- and pressure constancy was reached faster from one to the other adsorption or desorption step of the isotherms. This appears to be in accordance with the reduced mesopore volume (see above). The enhanced kinetics may also have to be seen in the light of more unblocked surface area of the zeolite crystals because of the missing binder in the beads. This behaviour of the molecular sieves also improves the performance of the storages. Further investigations are planned to deepen these findings.



Figure 2. Photograph of the thermal adsorption storage (open system).

Table 1. Comparison of the adsorption capacities in g/g of binderless and ordinary zeolite types A and X, TG upon adsorption at 298 K and RH 33%.

Zeolite	Isotherms at 298 K and RH = 33%	TG, desorption up to 723 K	TG, desorption up to 473 K
4ABF	0.250	0.266	0.200
4AK	0.220	0.231	0.180
13XBF	0.320	0.316	0.218
13XK	0.275	0.260	0.187

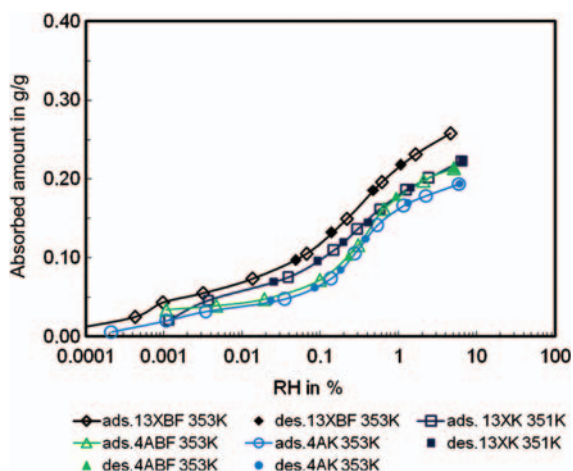


Figure 3. Water adsorption isotherms for 13XBF, 13XK, 4ABF and 4AK as a function of RH (calculated from the measured water vapour pressure); filled symbols denote desorption.

Not only the adsorption capacities and kinetics of the zeolites are important issues but also the hydrothermal stability of these materials. The stability of the binderless materials and the standard molecular sieves has been proven in cyclic adsorption/desorption measurements for closed- and open-system conditions. The results are summarized in Figures 4 and 5.

At a glimpse, both figures illustrate very similar results, despite different conditions applied in the tests (cf. figure captions). The known differences of the adsorption capacities for the A/X-zeolites and for the binderless-/standard zeolites discussed previously appear in this set of test results as well.

A-type beads show strong stability whatever conditions have been chosen in this study. It has to be mentioned that even application of $T = 350^{\circ}\text{C}$ and a water vapour pressure ($p_{\text{H}_2\text{O}}$) of up to 1000 mbar (open conditions) did not harm the zeolite structures of 4ABF and 4AK. The 13XK shows some degradation, but 13XBF is not stable at those conditions. The extension of the tests under closed conditions to actual 450 cycles shows for 13XBF a decrease in the adsorption capacity by one-third, whereas the capacity of 4ABF stays still constant.

Usually, the hydrothermal stability of zeolites depends on the Si/Al ratio, the nature of cations, the lattice type and the size of the cavities [9, 10]. Thus, it is not surprising to get the highest hydrothermal stability for the Na-forms of the A-zeolites we employ here [9]. According to Lutz *et al.* [10], some lower hydrothermal strength of zeolite X could be expected. The relatively low hydrothermal stability of 13XBF (compared with 13XK) at high temperatures and high water vapour pressures, however, cannot be explained yet in terms of the upper mentioned parameters.

Finally, the adsorption and storage behaviour of some selected samples have been investigated in the closed storage apparatus as well as in the open storage. The results are summarized in Table 2 and in Figures 6 and 7. The latter show changes of different parameters such as temperature, water vapour pressure or RH vs. time for 13XBF as an example. In general, the results of both systems give a similar picture.

Figure 6 illustrates the temperature profiles and the water vapour pressure upon discharging of the closed storage. The three uppermost curves show the temperatures in the storage material at different positions followed by the temperature of the storage/heat exchanger.

The differences of the three uppermost temperature curves indicate problems in delivering sufficient water vapour by the

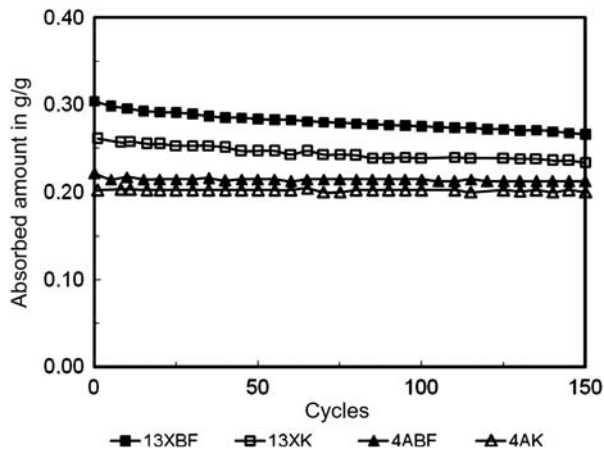


Figure 4. Hydrothermal stability in cycles adsorption/desorption under closed (vacuum) system conditions for binderless and standard zeolites. $T = \text{ambient}/350^{\circ}\text{C}$, $p_{\text{H}_2\text{O}} = 17 \text{ mbar}$.

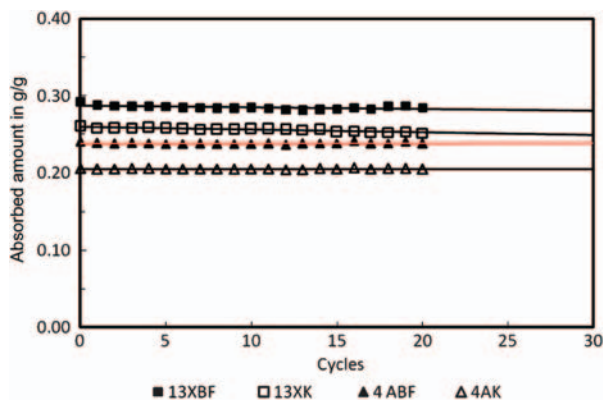


Figure 5. Hydrothermal stability in cycles adsorption/desorption under open-system conditions for binderless and standard zeolites, $T = 23^{\circ}\text{C}/200^{\circ}\text{C}$, $p_{\text{H}_2\text{O}}$ up to 1000 mbar, lines are trends.

Table 2. Results of the storage tests in open and closed systems, adsorbed amount after desorption at 200°C .

Zeolite	Kind of storage	T_{max} zeolite in $^{\circ}\text{C}$	Adsorbed amount in g/g
4ABF	Closed	120	0.180
13XBF	Closed	105	0.220
13XK	Closed	97	0.200
4ABF	Open	100	0.198
13XBF	Open	120	0.204

vaporizer because of the fast kinetics of 13XBF. This observation could not be made for the binder-containing materials (13XK, not shown). The temperature profiles were more or less identical over the entire volume of the storage material.

The dotted line in Figure 6 shows the progress of the water vapour pressure reaching the value of the vaporizer (kept at 20°C) at the end of the experiment.

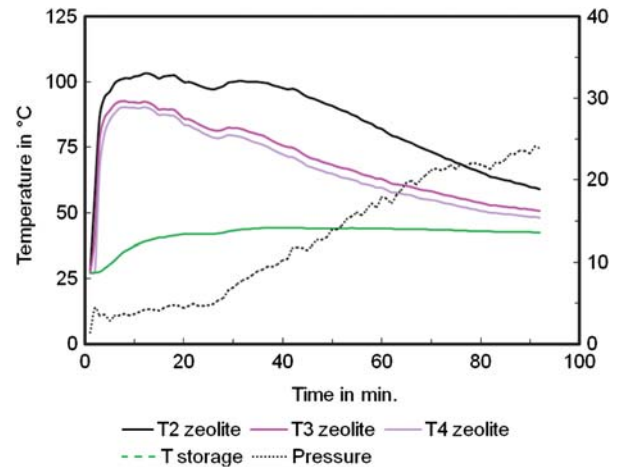


Figure 6. Temperature profiles in the storage and water vapour pressure in mbar (right-hand side axis) vs. time in the closed system for 13XBF.

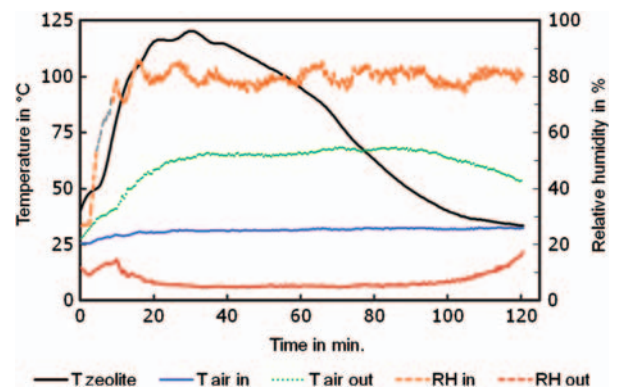


Figure 7. Temperature profiles and RH values of air in and out vs. time, open storage for 13XBF.

Figure 7 gives information about the temperature profiles and the RH values upon discharging of the open storage. Humid air enters the storage and much less humid air leaves the apparatus. The corresponding partial pressure of the water vapour in the feed air amounts to $\sim 35 \text{ mbar}$.

The temperature of the exiting air of the storage reaches 70°C for the 13XBF and 60°C for the 4ABF. This is a significant higher temperature than that obtained with the closed storage due to the known problems in heat transfer.

Table 2 compares the maximum temperatures measured in the zeolite bed and the adsorbed amounts determined after the experiments. Because the charging temperature of both storages (desorption of the zeolites) did not exceed 470 K, the adsorbed amounts match satisfactorily the TG values determined at 473 K (cf. Table 1, column 4). So, $\sim 70\text{--}75\%$ of the total adsorption capacity (cf. columns 3 and 4 in Table 1) can be utilized under those conditions. Accordingly, the storage densities or specific energies range between 130 and 165 Wh/kg for 4ABF and 13XBF, respectively. The standard X-zeolite showed a 6% lower specific energy.

4 CONCLUSIONS

We succeeded in manufacturing zeolite beads of types A and X free of any binder. These novel binderless molecular sieves are characterized by 10–15% higher adsorption capacities, faster kinetics and therefore potentially higher performance densities.

The hydrothermal stability of A-type products is excellent, whereas X-type materials show degradation effects at high temperatures and high water vapour pressures.

The binderless 13XBF zeolite is a promising storage material for charging temperatures up to 470 K, despite the reduced hydrothermal stability found for harsh conditions. For higher charging temperatures, however, the more stable binderless zeolite 4ABF is the better choice in open and closed storage systems.

ACKNOWLEDGEMENTS

We thank H. Stach and D. Ackermann (ZeoSolar e.V., Berlin) for their contributions to this study and D. Rohländer (Fraunhofer IKTS, Hermsdorf) for the SEM images. The financial support by the German Federal Ministry of Economics and Technology, grant number 0327439B, is acknowledged.

REFERENCES

- [1] Jänchen J, Ackermann D, Stach H. Adsorption properties of aluminophosphate molecular sieves—potential applications for low temperature heat utilization. In Wang RZ, Lu Z, Wang W, *et al.* (eds). *Proceedings of the International Sorption Heat Pump Conference (ISHPC) 2002*, 24–27 September 2002, Shanghai, PR China, 2002, 635–8.
- [2] Kakiuchi H, Takewaki T, Fujii M, *et al.* Adsorption heat pump, and use of adsorption material as adsorption material for adsorption heat pump. European Patent Application, EP 1 363 085 A1, 2002.
- [3] Jänchen J, Ackermann D, Stach H, *et al.* Studies of the water adsorption on zeolites and modified mesoporous materials for seasonal storage of solar heat. *Sol Energy* 2004;76:339–44.
- [4] Jänchen J, Stach H, Hellwig U. Water sorption in faujasite- and chabazite type zeolites of varying lattice composition for heat storage applications. In Gédéon A, Massiani P, Babonneau F (eds). *Proceedings of 4th International FEZA Conference on Zeolites and Related Materials*, 2–6 September 2008, Paris, France, *Studies in Surface Science and Catalysis*, Elsevier, Amsterdam, Vol. 174, 2008, 599–602.
- [5] Bauer J, Herrmann R, Mittelbach W, *et al.* Zeolite/aluminum composite adsorbents in adsorption refrigeration. *Int J Energy Res* 2009; 33:1233.
- [6] Hauer A. Thermochemical energy storage in open systems—temperature lift, coefficient of performance and energy density. In *Proceedings Terrastock 2000, 8th International Conference on Thermal Energy Storage*, 28 August–1 September 2000, Stuttgart, Germany.
- [7] Hauer A. Beurteilung fester Adsorbentien auf der Basis der Adsorptionsgleichgewichte für energetische Anwendungen in offenen Systemen. *Chemie Ingenieur Technik* 2010;82:1075–80.
- [8] Schumann K, Unger B, Brandt A, *et al.* Investigation on the pore structure of binderless zeolite 13X shapes. *Microporous Mesoporous Mater* 2012, in press, doi:10.1016/j.micromeso.2011.07.015.
- [9] Fichtner-Schmittler H, Lutz W, Amin S, *et al.* Hydrothermal damage of ion-exchanged A-type zeolite cation-directed mechanisms of phase transformation. *Zeolites* 1992;12:750–5.
- [10] Lutz W, Toufar H, Kurzhals R, *et al.* Investigation and modelling of the hydrothermal stability of technically relevant zeolites. *Adsorption* 2005;11: 405–13.